The structure of I cannot be too dissimilar from that of II, in the sense that the interchain interactions are developed presumably through NO-NO contact but keeing the two-dimensional structure. This is unfortunate, because the interaction is antiferromagnetic, and ferromagnetic three-dimensional order cannot be achieved in this way.

However, this does not mean that the use of carboxylates cannot lead to molecular based ferromagnets. Indeed we have observed relatively high transition temperatures[9] to three-dimensional magnetic order in $[Mn(pfbz)_2]_2$(NITR). The fact that we could not obtain suitable single crystals made the analysis of the magnetic phase transition not unambiguous, but there is an indication for either a weak ferro or ferrimagnetic transition. We can now suggest that $[Mn(pfbz)_2]_2$(NITR) has a two-dimensional structure which can be obtained from that of II, by substituting each NITMe-IMHMe conjugate pair with one NITR radical. In this way the scheme of magnetic structure given in Figure 5b would ensure a two-dimensional ferrimagnetic structure. The relatively high transition temperature observed in this case, in the range 20-25 K,[9] compared to that of the one-dimensional materials,[5,7] in the range 4-8 K, would be justified by the increased magnetic dimensionality.

Acknowledgment. The financial support of the CNR, of the Progetto Finalizzato "Materiali Speciali per Tecnologie Avanzate", and of MURST is gratefully acknowledged.

Supplementary Material Available: Tables SI-SV, listing crystallographic and experimental parameters, calculated positions of hydrogen atoms, anisotropic thermal factors, and bond distances and angles, and Figure S1, showing a schematic view of the puckered planes formed by hydrogen bonds (9 pages); Table SVI, listing observed and calculated structure factors (9 pages). Ordering information is given on any current masthead page.

Contribution from the Department of Physics, The Pennsylvania State University, University Park, Pennsylvania 16802, and the Departments of Chemistry, University of Southern California, Los Angeles, California 90089-0744, and University of Notre Dame, Notre Dame, Indiana 46556

Mossbauer and Magnetic Susceptibility Investigation of a Ferromagnetically Coupled Iron(III) Porphyrin-Dicopper(II) System with Imidazolate Bridging Ligands

Govind P. Gupta,[†,‡] George Lang,*[,†] Carol A. Koch,[§] Bing Wang,[§] W. Robert Scheidt,[∥] and Christopher A. Reed*[,§]

Received March 22, 1990

Susceptibility and Mossbauer techniques were employed to analyze the magnetic properties of the trinuclear complex $[Fe^{III}(TPP)(CuIM)_2]B_{11}CH_{12}\cdot 5THF$ (TPP = tetraphenylporphyrinate; CuIM = copper(II) complex of the Schiff base formed by sequential condensation of 5-chloro-2-hydroxybenzophenone, 1,2-diaminobenzene, and imidazole-4-carbaldehyde). The Fe(II) analogue (magnetic Fe(III) ions replaced by diamagnetic Fe(II) ions) and its Ni analogue (magnetic Cu ions replaced by diamagnetic Ni ions) were studied. Susceptibility measurements on the Fe(II) analogue in 10-kG magnetic field showed that the effective magnetic moment above 20 K remains 2.60 μ_B, which would correspond to two Cu ions with $S = {}^1/_2$ and $g_{Cu} = 2.12$. The magnetic moment below 20 K decreases significantly and was fitted with pairwise antiferromagnetic coupling with $J_{CuCu} = -1.52$ cm^{-1}. The diamagnetic character of Fe(II) was confirmed by Mossbauer spectroscopy. In the Ni analogue, $[Fe^{III}(TPP)(NiIM)_2]B_{11}CH_{12}\cdot 5THF$, the effective magnetic moment at 300 K is 2.2 μ_B and remains around 2 μ_B down to 2 K. The susceptibility and Mossbauer data were fitted with a $S = {}^1/_2$ model with axial field $\Delta/\lambda = 5$, rhombicity $V/\Delta = 0.4$, and one-electron spin-orbit coupling constant $\lambda = 400$ cm^{-1}, corresponding to $g_{Fe} = 1.63$, 2.14, and 2.90. The analysis of its Mossbauer spectra also provides $\delta = 0.24$ mm/s, $\Delta E = -2.26$ mm/s, $\eta = 0.1$ (where the principal EFG axis is along the x magnetic axis), and $P\kappa/(g_N{}^*\mu_N) = 17.0$ T/unit spin. All parameters are consistent with the $S = {}^1/_2$ character of this system. The effective magnetic moment of 3.4 μ_B found for $[Fe^{III}(TPP)(CuIM)_2]B_{11}CH_{12}\cdot 5THF$ at 300 K corresponds to a susceptibility that is the sum of those of its two analogues. However, as the temperature is decreased, the effective moment rises to a maximum at 8 K, indicating ferromagnetic Fe-Cu coupling. This can be understood in terms of a σ/π orthogonality of the magnetic orbitals. The analysis of the susceptibility data measured in the temperature range 2-300 K reveals ferromagnetic exchange of $J_{FeCu} = 22.2$ cm^{-1}, making a Cu-Fe-Cu type molecular spin, and an antiferromagnetic chainlike coupling of $J_{CuCu} = -1.87$ cm^{-1} between such molecular spins. High-field Mossbauer data are consistent with this interpretation. The zero-field Mossbauer parameters ($\delta = 0.23$ and $\Delta E = -2.07$ mm·s^{-1}) are very similar to those of the Ni analogue and are unaffected by spin coupling to copper.

Introduction

In a recent communication, we reported the first example of ferromagnetic coupling via an imidazolate bridging ligand.[1] The significance of this result lies in its support for the concept of orthogonal magnetic orbitals,[2] which is becoming an increasingly powerful rationale for intramolecular ferromagnetic interactions. The system involves the bis coordination of a copper(II) imidazolate chelate (CuIM) to a low-spin iron(III) tetraphenylporphyrin cation to give the trimetallic unit shown in Figure 1. The ferromagnetic interaction arises from a σ/π symmetry mismatch of the $d_{x^2-y^2}$ orbital on copper and the d_{yz} orbital on iron. The magnitude of the coupling, $J_{FeCu} = +22$ cm^{-1}, is surprisingly large considering the >6-Å separation of the metal atoms.

In addition to the intramolecular ferromagnetic interaction, there is an antiferromagnetic interaction between cations in the lattice, which adds a complexity to the system. However, by the complementary application of magnetic susceptibility measurements and Mossbauer spectroscopy, an overall magnetic coupling model can be developed. The details of this analysis are the main subject of this report. A number of features of the electronic structure of the system emerge from the analysis, and a linear-chain intermolecular interaction is required to rationalize the antiferromagnetic coupling component.

The broader significance of this work lies in its relation to models for the heme a_3/Cu_B site of cytochrome oxidase. MCD measurements on the cyanide form of this enzyme have been interpreted in terms of ferromagnetic coupling between iron(III) and copper(II),[3] and this conclusion is consistent with Mossbauer results.[4] A σ/π orthogonality of magnetic orbitals with respect

[†] The Pennsylvania State University.
[‡] On leave from Lucknow University, Lucknow, India.
[§] University of Southern California.
[∥] University of Notre Dame.

(1) Koch, C. A.; Reed, C. A.; Brewer, G.; Rath, N. P.; Scheidt, W. R.; Gupta, G. P.; Lang, G. *J. Am. Chem. Soc.* **1989**, *111*, 7645.
(2) Kahn, O.; Galy, J.; Journaux, Y.; Jaud, J.; Morgenstern-Badarau, I. *J. Am. Chem. Soc.* **1982**, *104*, 2165.
(3) Thomson, A. J.; Johnson, M. K.; Greenwood, C.; Gooding, P. E. *Biochem. J.* **1980**, *193*, 687.

0020-1669/90/1329-4234$02.50/0

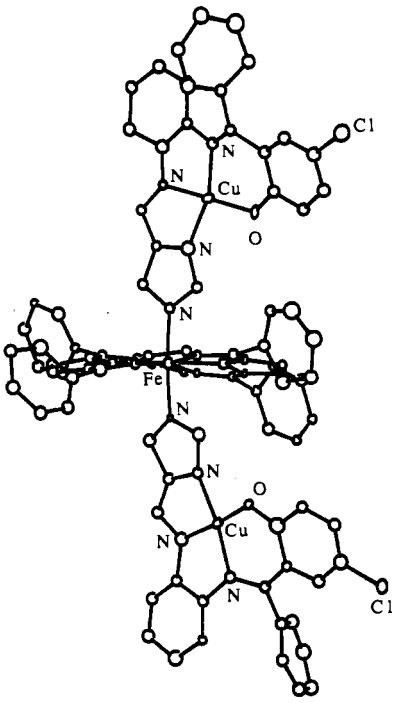

Figure 1. Perspective view of the [Fe(TPP)(CuIM)$_2$]$^+$ cation. CuIM is the copper(II) complex of the Schiff base formed by sequential condensation of 5-chloro-2-hydroxybenzophenone, 1,2-diaminobenzene, and imidazole-4-carbaldehyde. The representation of the trimetallic unit is taken from the X-ray structure reported in ref 1.

to a Fe–CN–Cu bridge provides[5,6] an appealing rationale for the sign of this magnetic interaction, i.e., J positive, and in the light of the present results the magnitude ($J > 100$ cm^{-1})[7] does not seem unreasonable.

Experimental Section

Fe(TPP)(THF)$_2$,[8] Fe(TPP)(B$_{11}$CH$_{12}$),[9] NiIM,[10] and CuIM[10] were prepared as previously described. All reactions were carried out in a Vacuum Atmospheres Corp. glovebox (O_2, H_2O < 1 ppm) with solvents that were dried and deoxygenated by distillation from sodium/benzophenone, except for dimethylformamide, which was vacuum-distilled but not dried. Except where noted, elemental analyses (including Fe/Cu and Fe/Ni ratios) and identifying λ_{max} data appear in the earlier communication, as do the details of the X-ray structural analysis.[1]

Fe(TPP)(NiIM)$_2$·2tol (tol = toluene) was prepared by mixing hot, filtered toluene solutions (25 mL) of Fe(TPP)(THF)$_2$ (0.050 g, 0.062 mmol) and NiIM (0.056 g, 0.122 mmol). After being heated for 5 min, the solution was set aside to crystallize overnight. The large cubic crystals formed were filtered off and rinsed with heptane (0.075 g, 70%). Magnetic susceptibility measurements showed weak paramagnetism (μ = 0.5 ± 0.1 μ_B between 6 and 300 K) ascribed to the 1–2% impurity, a feature also seen in the NiIM starting material. It could not be removed by recrystallization from toluene. Fe(TPP)(CuIM)$_2$·2tol was prepared in a similar manner in 50% yield.

[Fe(TPP)(CuIM)$_2$]B$_{11}$CH$_{12}$·5THF was prepared by heating Fe(TPP)(B$_{11}$CH$_{12}$)·2THF (0.036 g, 0.038 mmol) and CuIM (0.045 g, 0.097 mmol) in THF (20 mL) for 2 min. After the solution was filtered through a fine frit, heptane was allowed to diffuse into the solution to precipitate the product (0.069 g, 88%). [Fe(TPP)(NiIM)$_2$]B$_{11}$CH$_{12}$·5THF was prepared in a similar manner in 53% yield. It was possible to recrystallize small amounts of [Fe(TPP)(CuIM)$_2$]B$_{11}$CH$_{12}$ by diffusion of toluene into a saturated DMF solution. In this manner, a few single crystals suitable for X-ray analysis were obtained.[1] Since the detailed Mossbauer and susceptibility analyses were done on the more readily available tetrahydrofuran solvate, sufficient amounts of the dimethylformamide solvate were accumulated to test for possible differences in the magnetic properties of the two lattices. The X-ray analysis of the dimethylformamide solvate suggested an approximate 3DMF·3H$_2$O solvate composition, leading to an expected elemental analysis of C$_{100}$H$_{97}$N$_{15}$B$_{11}$C$_{12}$Cu$_2$FeO$_8$: C, 59.76; H, 4.86; N, 10.45. Found: C, 64.99; H, 4.52; N, 8.82. The found values can be fitted to a variety of mixed-solvate formulations, all of which replace a considerable portion of the DMF and H_2O with toluene. This uncertainty in the molecular weight does not significantly perturb the susceptibility calculations and is not incompatible with the solvate volume and solvate disposition seen in the X-ray structure (R = 14.4%).[1]

Magnetic susceptibility data were acquired on an SHE 905 SQUID susceptometer at 10 kG by using finely ground samples (30 mg) pressed into a precalibrated aluminum bucket. Mossbauer spectra were run on polycrystalline samples immobilized in melted paraffin wax. Spectra were recorded in a horizontal transmission geometry as detailed elsewhere.[11]

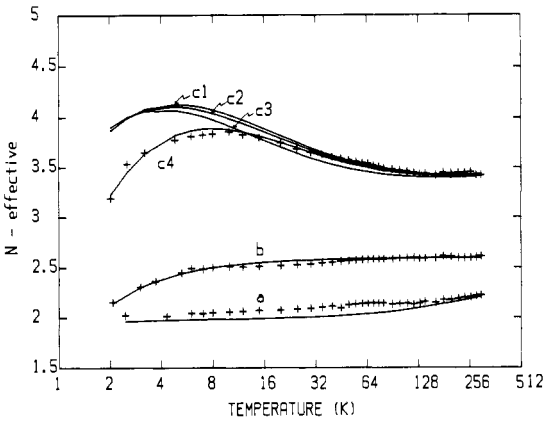

Figure 2. Experimental values of N_{eff} as a function of temperature, where $N_{eff} = (3kT\chi_M/N\mu_B^2)^{1/2}$ and χ_M is the susceptibility per heme unit, plotted as +'s. The solid curves correspond to calculations. Key: (a) [Fe^{III}(TPP)(NiIM)$_2$]B$_{11}$CH$_{12}$·5THF, solid curve corresponds to Δ/λ = 5, V/λ = 2, and λ = 400 cm^{-1}; (b) [Fe^{II}(TPP)(CuIM)$_2$]·2tol, solid curve corresponds to J_{CuCu} = −1.52 cm^{-1}; (c1–4) [Fe^{III}(TPP)(CuIM)$_2$]B$_{11}$CH$_{12}$·5THF, solid curves correspond to the crystal field parameters given in (a) and (c1) J_{FeCu} = 22.2 cm^{-1} and J_{CuCu} = 0 cm^{-1}, (c2) J_{FeCu} = 22.2 cm^{-1} and J_{CuCu}(intramolecular) = −1.52 cm^{-1}, (c3) J_{FeCu} = 15.4 cm^{-1} and J_{CuCu} = 0 cm^{-1}, and (c4) J_{FeCu} = 22.2 cm^{-1} and J_{CuCu}(intermolecular) = −1.87 cm^{-1}.

Results, Analysis, and Discussion

Susceptibility. In order to emphasize the interesting low-temperature region, a log temperature scale (to the base 2) has been used. The magnetic susceptibility is indicated in terms of the effective Bohr magneton number, symbol N_{eff}. This is unambiguously related to the susceptibility by $N_{eff} = (3kT\chi_M/N\mu_B^2)^{1/2}$. The abbreviation DIA is used for the diamagnetic susceptibility, TDP for temperature-dependent paramagnetism, and TIP for temperature-independent paramagnetism.

[Fe^{II}(TPP)(CuIM)$_2$]·2tol. The magnetic moment of this complex was measured in a 10-kG magnetic field over a temperature range 2–300 K. The high-temperature susceptibility data were normalized to Curie paramagnetism, yielding a diamagnetic and temperature-independent paramagnetic correction DIA + TIP(Cu) = −905 × 10^{-6} cgsu. The corresponding values of N_{eff} for TDP(Cu) are plotted as the middle data set (b) in Figure 2. The high-temperature (>20 K) value of N_{eff} = 2.60 corresponds to two Cu ions with $S = {}^1/_2$ and g_{Cu} = 2.12. The assumed diamagnetic nature of Fe(II) centers was confirmed by Mossbauer spectra over the temperature range 4.2–195 K in 6-T magnetic field.

The significant decrease in N_{eff} below 20 K suggests antiferromagnetic coupling between Cu ions. The data were fitted with a standard isotropic spin interaction ($\mathcal{H} = -J\tilde{S}_1\cdot\tilde{S}_2$), as indicated

(4) Kent, T. A.; Munck, E.; Dunham, W. R.; Filter, W. F.; Findling, K. L.; Yoshida, T.; Fee, J. A. *J. Biol. Chem.* **1982**, *257*, 12489.
(5) Thomson, A. J.; Greenwood, C.; Gadsby, P. M. A.; Peterson, J.; Eglinton, D. G.; Hill, B. C.; Nicholls, P. *J. Inorg. Biochem.* **1985**, *23*, 187.
(6) Kahn, O. *Struct. Bonding* **1987**, *68*, 89.
(7) The triplet–singlet energy gap is estimated to be >200 cm^{-1}.[3]
(8) Reed, C. A.; Mashiko, T.; Scheidt, W. R.; Spartalian, K.; Lang, G. *J. Am. Chem. Soc.* **1980**, *102*, 2302.
(9) Gupta, G. P.; Lang, G.; Lee, Y. J.; Scheidt, W. R.; Shelly, K.; Reed, C. A. *Inorg. Chem.* **1987**, *26*, 3022.
(10) Brewer, C. T.; Brewer, G. A. *Inorg. Chem.* **1987**, *26*, 3420.
(11) Lang, G.; Dale, B. W. *Nucl. Instrum. Methods* **1974**, *116*, 567.

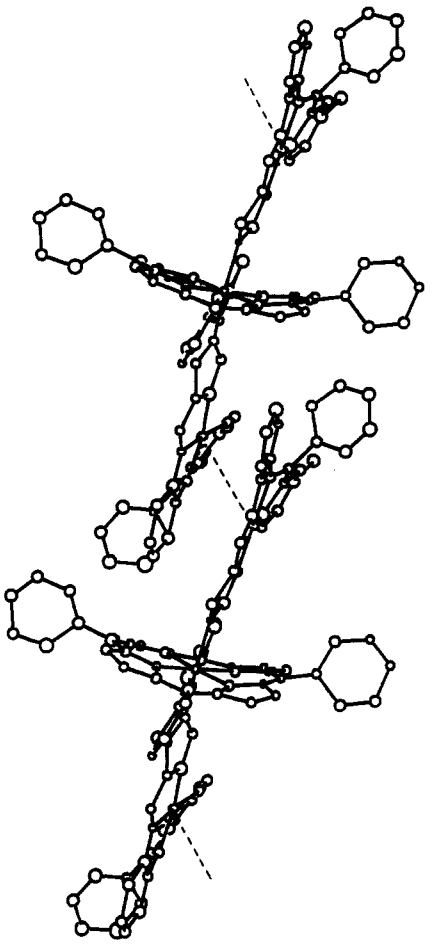

Figure 3. Perspective view of the cations in the X-ray crystal structure of $[Fe^{III}(TPP)(CuIM)_2]B_{11}CH_{12}$, showing the development of a linear-chain-type intermolecular effect. The dotted line indicates the proposed intermolecular Cu···Cu interaction.

by the solid line in Figure 2b. The model treats coupling by pairs, with $J_{CuCu} = -1.52$ cm^{-1}. The intramolecular Cu···Cu separation in $Fe(TPP)(CuIM)_2$ must be ca. 12–13 Å, since these paramagnetic centers are connected by two imidazolate ligands and the diamagnetic iron atom. While antiferromagnetic coupling across such a long distance is not unreasonable, in the absence of a crystal structure it is not possible to distinguish intramolecular coupling from possible intermolecular coupling. In fact, the structure of the corresponding iron(III) species shows a slipped, face-to-face relationship of copper chelates between adjacent molecules, and a coupling model with $J_{CuCu} = -1.87$ cm^{-1} has been developed (see below and Figure 3). The large disklike shape of the CuIM ligands makes it likely that ring stacking will be a feature of all lattices with compounds of the present structural type.

$[Fe^{III}(TPP)(NiIM)_2]B_{11}CH_{12}\cdot 5THF$. Only iron contains unpaired spin in this complex. The N_{eff} value near 2.1 over the entire temperature range is consistent with a low-spin ferric ion. Since the ground-state doublet is not completely isolated, the iron susceptibility does not necessarily follow Curie law behavior even at temperatures around 300 K. At the same time, the paramagnetism is fairly small. This makes the magnitude of the DIA + TIP(Ni) correction important, particularly in calculating the true TDP(Fe) at high temperature. Fortunately, we have available, from our Mossbauer measurements on this complex, the crystal field splittings of the ferric ion and are able to calculate its TDP and TIP. Iron susceptibility dominates this complex at low temperatures, and there our calculated values fit the data with any reasonable correction for the remainder of the molecule. In the interests of clarity we delay justification for our correction methods, but we have concluded that DIA + TIP(Ni) in the present case should closely approximate DIA + TIP(Cu) in

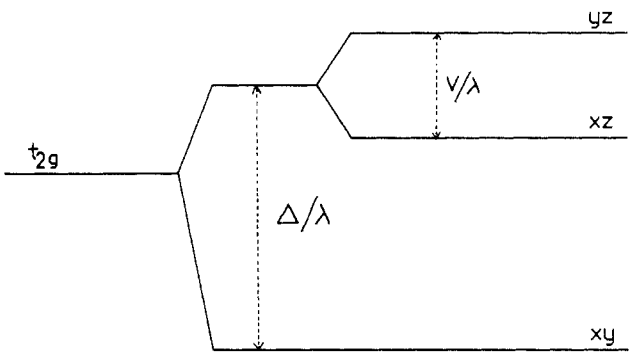

Figure 4. Diagram of t_{2g} electron energy levels shown for crystal field parameters $\Delta/\lambda = 5$ and $V/\lambda = 2$.

$[Fe^{III}(TPP)(CuIM)_2]B_{11}CH_{12}\cdot 5THF$. We use the same correction, -950×10^{-6} cgsu units, in both cases. The bottom data points of Figure 2 have been so corrected, and the N_{eff} values represent the iron contribution (TIP + TDP) only.

The iron susceptibility is related to the crystal field parameters by using the model of Griffith,[12] later extended to Mossbauer spectroscopy by Lang and Marshall.[13] In this model the octahedral crystal field is assumed large, isolating the three low-lying t_{2g} orbitals from the e_g. Lower symmetry crystal fields split the t_{2g}, with the splittings parametrized by V and Δ as shown in Figure 4. The original system states, formed by the three possible arrangements of five d electrons in t_{2g}, are mixed by spin–orbit interaction according to the Hamiltonian

$$\mathcal{H}_c = \sum[\mathcal{V}(\vec{l}_i) + \lambda\vec{l}_i\cdot\vec{s}_i] \quad (1)$$

where the summation extends over the d electrons. In the Hamiltonian λ is the one-electron spin–orbit interaction constant and $\mathcal{V}(\vec{l}_i)$ is the crystal field.

The Hamiltonian (eq 1), with addition of the Zeeman magnetic interaction term

$$\mathcal{H}_m = \mu_B\vec{H}_{ap}\cdot\sum(2\vec{s}_i + \vec{l}_i) \quad (2)$$

provides a satisfactory fit to the experimental data (shown in Figure 2a) with $\Delta/\lambda = 5$, $V/\lambda = 2$, and $\lambda = 400$ cm^{-1}. The susceptibility data do not unambiguously determine these crystal field parameters; they have been obtained from the Mossbauer analysis discussed in the next section.

$[Fe^{III}(TPP)(CuIM)_2]B_{11}CH_{12}\cdot 5THF$. In this system the Ni atoms are replaced by Cu, so that we now have one iron and two copper sites, each with one unpaired spin in the molecule. We assume that the intrinsic natures of the Fe(III) and Cu sites are unchanged from the previously discussed "diamagnetic control" complexes. A maximum of N_{eff} at about 8 K suggests an intramolecular ferromagnetic coupling between Fe and the two nearby Cu ions. At high temperatures, where Fe–Cu and Cu–Cu spin coupling may be neglected, we are able to calculate the iron susceptibility and TDP(Cu). The remainder, DIA + TIP(Cu), we have adjusted to -950×10^{-6} cgsu to fit both the present sample and $[Fe^{III}(TPP)(NiIM)_2]B_{11}CH_{12}\cdot 5THF$, as indicated above. The remaining susceptibility, TDP(Fe) + TIP(Fe) + TDP(Cu), is represented by the N_{eff} values shown as the top set of data points in Figure 2.

We now have the problem of determining the spin-coupling parameters for our complex. In our initial effort, each molecule was treated as an internally coupled spin system acting independently of its neighbors according to the Hamiltonian

$$\mathcal{H} = \mathcal{H}_c + \mathcal{H}_m - \mu_B g_{Cu}\vec{H}_{ap}\cdot(\vec{S}_{Cu1} + \vec{S}_{Cu2}) - J_{FeCu}\vec{S}_{Fe}\cdot(\vec{S}_{Cu1} + \vec{S}_{Cu2}) \quad (3)$$

where the first two terms are the same as those in the case of $[Fe^{III}(TPP)(NiIM)_2]B_{11}CH_{12}\cdot 5THF$, the third term represents the Zeeman magnetic interaction of the two Cu atoms, and the

(12) Griffith, J. S. *Nature (London)* **1957**, *180*, 30.
(13) Lang, G.; Marshall, W. *Proc. Phys. Soc.* **1966**, *87*, 3.

last term represents the Cu–Fe–Cu exchange interaction. For simplicity, and in view of the symmetric crystal structure, the exchange interactions between iron and the two Cu spins were considered to be the same.

With J_{FeCu} near 20 cm^{-1}, this model could reproduce the initial increase of N_{eff} with falling temperature but not its subsequent decrease in the very low temperature range. This suggested the presence of an antiferromagnetic Cu–Cu coupling, as was seen in $Fe^{II}(TPP)(CuIM)_2\cdot 2tol$. We inserted an additional term $-J_{CuCu}(\vec{S}_{Cu1}\cdot\vec{S}_{Cu2})$ into (3) in order to treat the interaction as intramolecular. However, in the presence of a large ferromagnetic interaction it has very little effect. Two theoretical curves corresponding to $J_{CuCu} = 0$ and -1.52 cm^{-1} with $J_{FeCu} = 22.2$ cm^{-1} are compared in Figure 2 (curves c1 and c2, respectively). We have considered stronger intramolecular Cu–Cu coupling as well; none provides a good fit to the data.

At this point, the crystal structure became available to us. It revealed a slipped, face-to-face relationship between copper chelates in neighboring $[Fe(TPP)(CuIM)_2]^+$ cations, giving, in effect, a linear-chain structure for the metal ions (see Figure 3). The interchelate mean plane spacing is 3.37 Å, and the intermolecular Cu···Cu separation is 4.13 Å. Although this feature was determined for a crystal grown from dimethylformamide, we believe the same feature obtains in the polycrystalline material grown from THF. First, the magnetic susceptibility and zero-field Mossbauer data from the DMF solvate, although less precise because of sample limitations, are the same within experimental error (~3%). Second, π–π stacking of rings is a very common feature of chelate structures and may be the dominating factor in determining the lattice structure. The solvates and anions presumably play a more minor role, filling the available space in the lattice. Some indirect evidence that this may be true comes from related work with Mn(TPP)(CuIM)·tol,[14] where indistinguishable unit cell dimensions are obtained as the solvent is varied from toluene to benzene.[15]

Intermolecular Cu–Cu interaction in the present case gives rise to a long-range interaction and poses considerable theoretical difficulty. Because coupling strengths are so different, it is a good approximation to regard this system at low temperature as a Heisenberg linear chain of spins $S = {}^3/_2$, with antiferromagnetic coupling described by $-J_H(\vec{S}_i\cdot\vec{S}_{i+1})$. We chose to approximate this by using results obtained by Fisher[16] for linear chains of infinite (i.e. unquantized) spin. He found that the coupling has the effect of multiplying the uncoupled susceptibility by a factor $f = [1 + u(K)]/[1 - u(K)]$, where $u(K) = \coth(K) - 1/K$ and $K = J/(2kT)$. Fisher's J is related to our coupling constant by $J = 2S(S + 1)J_H$. Where the uncoupled susceptibility of Fisher is the simple Curie law susceptibility of the individual sites, we used the value calculated from (3) above. This makes no difference at the low-temperature end, $kT \ll J_{FeCu}$, and correctly represents the behavior at $kT \gg J_H$, where the antiferromagnetic coupling is no longer important. The fit (c4) to the top data set of Figure 2 was achieved by setting $J_{FeCu} = 22.2$ cm^{-1} and $J_H = -0.21$ cm^{-1}. The latter value when cast in terms of Cu–Cu coupling corresponds to $J_{CuCu} = -1.87$ cm^{-1}. This can be compared with the value -1.52 cm^{-1} found for bare Cu spins in $[Fe^{II}(TPP)(CuIM)_2]\cdot 2tol$.

We now return to a discussion of our DIA + TIP corrections. The TIP contributions of transition-metal ions may be estimated by the relationship[17]

$$\text{TIP} = 4mN\mu_B^2/E \qquad (4)$$

where m is the number of holes in the 3d shell and E is the average energy gap between the ground and the excited states, which mix via the orbital angular momentum operator. For Cu, $m = 1$ and $E = 12600$ cm^{-1} (for four-coordinated planar complexes).[17] Thus,

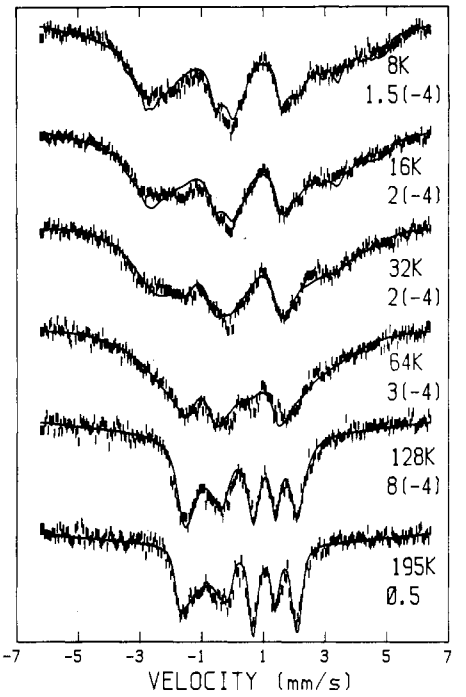

Figure 5. Mossbauer spectra of $[Fe^{III}(TPP)(NiIM)_2]B_{11}CH_{12}\cdot 5THF$ in 6-T field at temperatures as shown. The solid curves are the corresponding simulated spectra with $\Delta/\lambda = -4$, $V/\lambda = 4$, $\Delta = 2.26$ mm/s, $\delta = 0.24$ mm/s, $\Gamma = 0.23$ mm/s, $\eta = 0.1$, and $P_K/g_N\mu_N = 17.0$ T/unit spin. The values of w_0 in (mm/s) cm^3 are also shown in the figure along with temperatures for each spectrum. The numbers in the parentheses are the powers of 10 as a multiplying factor.

for each Cu we have a TIP of 80×10^{-6} cgsu. For Ni, $m = 2$ and $E = 22000$ cm^{-1} (for square-planar diamagnetic Ni compounds)[18] and we have a TIP of 90×10^{-6} cgsu for each atom. The orbital diamagnetism of the molecule as a whole is expected to be about 10 times these magnitudes, so it is a good approximation to neglect the small difference and use 80×10^{-6} cgsu for Ni as well. In $[Fe^{III}(TPP)(NiIM)_2]B_{11}CH_{12}\cdot 5THF$, the susceptibility contributed by iron could be calculated from Mossbauer information. The iron susceptibility and Cu $\tilde{g}$ components of $[Fe^{III}(TPP)(CuIM)_2]B_{11}CH_{12}\cdot 5THF$ were known from analogues. The coupling constants were determined by the low-temperature measurements, which are insensitive to diamagnetic correction. The net correction -950×10^{-6} cgsu fitted both complexes well, implying in each case a diamagnetic part of -1110×10^{-6} cgsu. This compares well with the value -1180×10^{-6} cgsu obtained by using -700×10^{-6} cgsu for TPP[19] and Pascal's constants[20] for the remaining atoms. The analogous calculation for the Fe(II) compound yields -937×10^{-6} cgsu; this acceptably approximates the -1065×10^{-6} value that our fit to experiment implies. We note that in all samples the calculated diamagnetism is subject to more cumbersome constitutive corrections.[20]

Mossbauer Spectra. Zero Field. Mossbauer spectra at 4.2 K in zero field provide isomer shifts $\delta = 0.24$ and 0.23 mm/s, quadrupole splittings $\Delta E = -2.26$ and -2.07 mm/s, and line widths $\Gamma = 0.67$ and 0.24 mm/s for $[Fe^{III}(TPP)(NiIM)_2]B_{11}CH_{12}\cdot 5THF$ and $[Fe^{III}(TPP)(CuIM)_2]B_{11}CH_{12}\cdot 5THF$, respectively. The values of δ and ΔE are consistent with low-spin ferric systems in both cases. The large line width in $[Fe^{III}(TPP)(NiIM)_2]B_{11}CH_{12}\cdot 5THF$ was attributed to relaxation effects, since it decreased as temperature increased. The sign of quadrupole splitting was determined in each case by applying a field of 6 T at 195 K. The line width in $[Fe^{III}(TPP)(NiIM)_2]B_{11}CH_{12}\cdot 5THF$ decreased to 0.23 mm/s under these conditions.

(14) Koch, C. A.; Wang, B.; Brewer, G.; Reed, C. A. *J. Chem. Soc., Chem. Commun.* **1989**, 1754.
(15) Unit cell constants for Mn(TPP)(CuIM)·xtol: $a = 16.58$ Å, $b = 27.56$ Å, $c = 29.13$ Å, $\alpha = 58.2°$, $\beta = 67.2°$, and $\gamma = 78.6°$. Unit cell constants for Mn(TPP)(CuIM)·x(benzene): $a = 16.46$ Å, $b = 27.85$ Å, $c = 29.44$ Å, $\alpha = 58.0°$, $\beta = 67.5°$, and $\gamma = 78.1°$.
(16) Fisher, M. E. *Am. J. Phys.* **1964**, *32*, 343.
(17) Griffith, J. S. In *The Theory of Transition Metal Ions*; University Press: Cambridge, England, 1971; p 280.
(18) Maki, G. *J. Chem. Phys.* **1958**, *29*, 1129.
(19) Eaton, S. S.; Eaton, G. R. *Inorg. Chem.* **1980**, *19*, 1095.
(20) Boudreaux, E. A.; Mulay, L. N. *Applications of Molecular Paramagnetism*; Wiley: New York, 1976.

$[Fe^{III}(TPP)(NiIM)_2]B_{11}CH_{12}\cdot 5THF$ in Magnetic Fields. Solution of the Hamiltonian $\mathcal{H}_c + \mathcal{H}_m$ ((1) and (2) above) yields system states that are linear combinations of five-electron Slater determinants. The ground doublet can be written as

$$|\Psi^+\rangle = a|1\alpha\rangle + b|\zeta\beta\rangle + c|-1\alpha\rangle$$

$$|\Psi^-\rangle = a|-1\beta\rangle - b|\zeta\alpha\rangle + c|1\beta\rangle \quad (5)$$

where each Slater determinant is named by the one-electron state that it leaves unoccupied and the coefficients a–c are determined by the crystal field. The orbital parts above are related to the usual t_{2g} by

$$|\pm 1\rangle = \mp(|xz\rangle \pm |yz\rangle)/\sqrt{2}$$

$$|\zeta\rangle = |xy\rangle \quad (6)$$

In order to conserve computer time, an $S = {}^1/_2$ spin-Hamiltonian formulation was adopted. Here the wave functions (5) are treated as a spin doublet and the Zeeman and hyperfine interactions of the true doublet are expressed in terms of appropriate $\tilde{\mathbf{g}}$ and $\tilde{\mathbf{A}}$ tensors, whose components are found by using the results of Lang and Marshall.[13]

$$g_x = 2[2ac - b^2 + \sqrt{2}b(c - a)]$$

$$g_y = 2[2ac + b^2 + \sqrt{2}b(c - a)]$$

$$g_z = 2[2a^2 - b^2] \quad (7)$$

$$A_x = 2g_N{}^*\mu_N P[2\sqrt{2}b(c - a) - \kappa(2ac - b^2) - {}^1/_7(2b^2 + 6c^2) - 3\sqrt{2}ab + 2ac - 3\sqrt{2}bc]$$

$$A_x = 2g_N{}^*\mu_N P[2\sqrt{2}b(c + a) - \kappa(2ac + b^2) - {}^1/_7(-2b^2 - 6c^2) + 3\sqrt{2}ab + 2ac - 3\sqrt{2}bc]$$

$$A_z = 2g_N{}^*\mu_N P[2(a^2 - c^2) - \kappa(a^2 - b^2 + c^2) + {}^2/_7(1 + b^2 - 3\sqrt{2}ab)] \quad (8)$$

Here P scales the orbital and dipolar hyperfine interactions and $P\kappa$ scales the contact interaction. The asterisks refer to the excited nuclear state; the same equations with asterisks removed apply to the ground state. The quadrupole field attributable to the d electrons is given by

$$QV_{zz}/4 = (0.5a^2 - b^2 + 0.5c^2)\Delta E_0/2$$

$$\eta = -3ac/(0.5a^2 - b^2 + 0.5c^2) \quad (9)$$

where ΔE_0 is the quadrupole splitting that an electron in a pure t_{2g} orbital state would produce.

In an applied field, the spin of each energy level can be found, by using the $\tilde{\mathbf{g}}$ tensor above. The Mossbauer spectrum is then determined from the nuclear Hamiltonian

$$\mathcal{H}_N = \vec{I}\cdot\tilde{\mathbf{A}}\cdot\langle\vec{S}\rangle + (QV_{zz}/4)\{I_z^2 - {}^5/_4 + (\eta/3)(I_x^2 - I_y^2)\} - g_N\mu_N\vec{H}_{ap}\cdot\vec{I} \quad (10)$$

by using the program of Lang and Dale.[11] In slow relaxation the Mossbauer spectrum is calculated for each electronic state and these are summed, with appropriate Boltzmann factors. In fast relaxation the thermal expectation value of spin is used as $\langle\vec{S}\rangle$, and a single Mossbauer spectrum is found.

The 4.2 K, 6 T spectrum was fitted by adjusting asymmetry parameter η, hyperfine coupling constant P, and crystal field parameters Δ/λ and V/λ. The latter were used to determine a–c, hence $\tilde{\mathbf{g}}$ and $\tilde{\mathbf{A}}$. Equations 9 were not used; quadrupole splitting, isomer shift, and line width were set at values found in zero field. The value of κ was assumed to be 0.35. The fitting provided $\Delta/\lambda = -4$, $V/\lambda = 4$, $\eta = 0.1$, and $P\kappa/g_N{}^*\mu_N = 17.0$ T/unit spin. The values of Δ/λ and V/λ correspond to quadrupole splitting, $0.5QV_{zz}(1 + \eta^2/3)^{1/2}$, and asymmetry parameter η equal to −2.69 mm/s and 0.09, respectively, by using relations (9) and taking ΔE_0 as 3.0 mm/s. These are in good agreement with the observed values, −2.26 mm/s and 0.1, respectively. The corresponding $\tilde{\mathbf{g}}$ components are −2.14, 2.90, −1.63. We note that none of our measurements relates our coordinate system to the molecular axes, and the EPR studies of several single-crystal low-spin ferric heme complexes indicate that largest $\tilde{\mathbf{g}}$ component is along the heme normal.[21] Since this is probably true for our sample, and usual convention is to take the heme normal to the z direction, we now relabel our axes so that our old y becomes z, z becomes x, and x becomes y. In this new scheme V_{zz} is positive (but not dominant), $\eta = -2.27$, $\Delta/\lambda = 5$, and $V/\lambda = 2$. The relabeled $\tilde{\mathbf{g}} = 1.63$, 2.14, and 2.90 are in fair agreement with $\tilde{\mathbf{g}} = 1.45$, 2.22, and 3.06 obtained by EPR study of the single crystals of cytochrome c.[22] The new x and y lie in the porphyrin plane, and the unpaired electron is in a yz orbital.

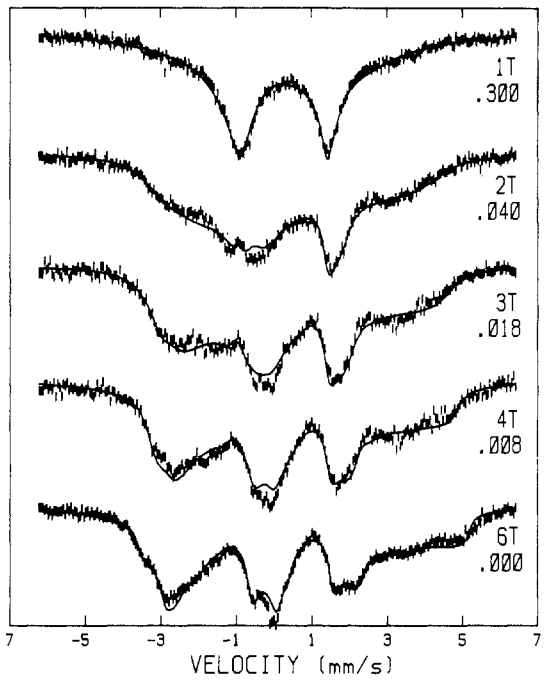

Figure 6. Mossbauer spectra of $[Fe^{III}(TPP)(NiIM)_2]B_{11}CH_{12}\cdot 5THF$ at 4.2 K in various applied fields as shown. The simulated spectra (solid curves) are calculated by using parameters given in Figure 5. The values of w_0 in (mm/s) cm^3 are given in the figure along with the applied fields.

The 4.2 K spectra recorded in low magnetic field seem to be in the intermediate relaxation regime and could be fitted with a modification based on a computer program written by Schulz and co-workers[23] as discussed in our earlier paper.[24] The program introduces a fluctuation matrix as

$$W_{ji} = w_0\Delta_{ij}{}^3/(\exp(\Delta_{ij}/kT) - 1) \quad (11)$$

with $\Delta_{ij} = E_i - E_j$, where w_0 may be treated as a free relaxation parameter. Since the observable effect of relaxation is to broaden the Mossbauer absorption lines, we prefer to define w_0 in units (mm/s) cm^3. This is convenient when the Mossbauer energy scale in mm/s is used and the electronic level separation is known in cm^{-1}.

All the spectra at various temperatures in a fixed field of 6 T (Figure 5) and in various fields at a fixed temperature 4.2 K (Figure 6) could be fitted successfully. The values of w_0 in different cases are given along with each spectrum shown in Figures 5 and 6.

$[Fe^{III}(TPP)(CuIM)_2]B_{11}CH_{12}\cdot 5THF$ in Magnetic Fields. In order to consider the coupling of Fe(III) with two neighboring

(21) Palmer, G. In *Iron Porphyrins 1983*; Addison-Wesley: Reading, MA, 1983; Vol. II, p 46.
(22) Taylor, C. P. S. *Biochim. Biophys. Acta* **1977**, *491*, 137.
(23) (a) Winkler, H.; Schulz, C.; Debruner, P. G. *Phys. Lett.* **1979**, *69A*, 360. (b) Schulz, C. Ph.D. Thesis, University of Illinois, 1979.
(24) Gupta, G. P.; Lang, G.; Scheidt, W. R.; Geiger, D. K.; Reed, C. A. *J. Chem. Phys.* **1986**, *85*, 5212.

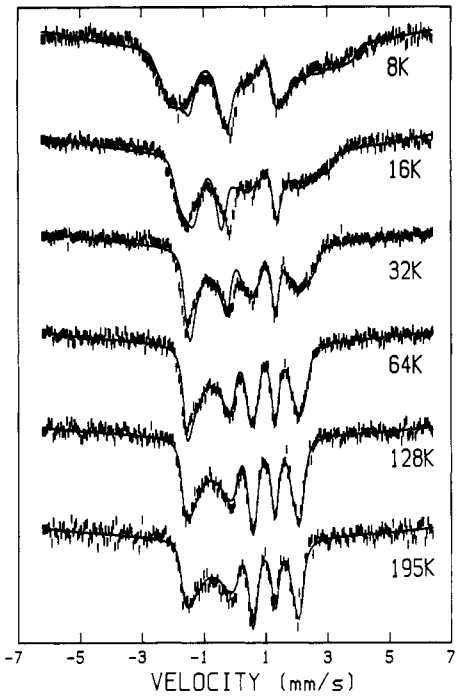

Figure 7. Mossbauer spectra of [Fe^{III}(TPP)(CuIM)$_2$]B$_{11}$CH$_{12}$·5THF in 6-T field at temperatures as shown. The solid curves are the corresponding simulated spectra in the fast relaxation limit with $\Delta/\lambda = -4$, $V/\lambda = 4$, $\Delta E = -2.07$ mm/s, $\delta = 0.23$ mm/s, $\Gamma = 0.24$ mm/s, $\eta = 0.1$, $P\kappa/g_N\mu_N = 17.0$ T/unit spin, $J_{FeCu} = 22.2$ cm^{-1}, and J_{CuCu}(intermolecular) = -1.87 cm^{-1}.

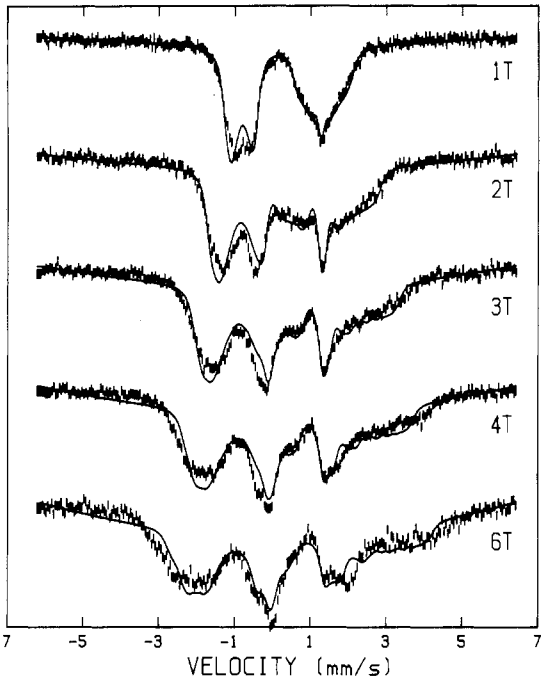

Figure 8. Mossbauer spectra of [Fe^{III}(TPP)(CuIM)$_2$]B$_{11}$CH$_{12}$·5THF at 4.2 K in various applied fields as shown. The simulated spectra (solid curves) are calculated by using parameters given in Figure 7.

Cu ions, the idea of fictitious $S = {}^1/_2$ for the iron was abandoned and a full Hamiltonian as given by eq 7 was employed. The expectation values of spin, orbital, and dipolar components, $\vec{S}$, $\vec{L}$, and $\vec{D}$, respectively, were calculated for Fe^{3+} and were further multiplied by the factor f to take into account the effect of intermolecular chain-type coupling. Once these values were known, the Mossbauer spectra were calculated by using Hamiltonian (10) with $\vec{A}\cdot\langle\vec{S}\rangle = g_N{}^*\mu_N P(\vec{L} + \vec{D} - \kappa\vec{S})$.

The zero-field 4.2 K Mossbauer spectra show that this complex relaxes much faster than its Ni analogue, so all the spectra were fitted in the fast relaxation limit. The spectra in Figures 7 and 8 are consistent with the intra- and intermolecular coupling constants J_{FeCu} and J_{CuCu} equal to 22.2 and -1.87 cm^{-1}, respectively.

Conclusion. The complementary application of susceptibility and Mossbauer studies, together with a knowledge of structure, allows a good quantitative description of the magnetic properties of spin-coupled iron(III)/copper(II) systems to be made. The study has profited greatly from the synthetic availability of "diamagnetic controls" where the paramagnetic iron(III) and copper(II) can in turn be replaced by diamagnetic iron(II) and nickel(II). The partitioning of intramolecular ferromagnetic effects from intermolecular antiferromagnetic effects, while dictated by conceptual convenience, is seen to be realistic. While it is possible that the magnitude of the unique ferromagnetic coupling in the Fe–imidazolate–Cu moiety may be overestimated by treating it as a localized effect, the order of magnitude difference in strength of the localized effect versus the linear-chain effect would seem to justify the conclusions. The propagation of moderately strong ferromagnetic interactions over large distances (~6 Å) presents interesting possibilities for the synthesis of ordered polymeric materials.

We also make the general observation that spin coupling of copper to an iron porphyrin, while it may alter the relaxation rates and other subtle features, does not alter the diagnostic isomer shift and quadrupole splitting that are commonly used to identify spin state and oxidation state. Thus, all species reported in this work have zero-field Mossbauer parameters that are entirely typical of their well-known bis(imidazole)iron(III) porphyrin complexes.[25] The same observation has been made for spin coupling of radicals to iron(III) porphyrins[26] and spin coupling of an iron–sulfur cube to a siroheme in sulfite reductase.[27] It leads us to question the formulation of a presumed Cu^{II}–O–Fe^{III}(TPP) species whose Mossbauer parameters ($\delta = 0.23$, $\Delta = 2.06$ mm s^{-1} at 136 K)[28] are much more consistent with bis(imidazole) low-spin species than the proposed intermediate-spin species.

Conceptually related CuIM complexes of chromium(III) tetraphenylporphyrin[29] and a possibly related manganese(III) system[30] have very recently been reported.

Acknowledgment. We thank Dr. Greg Brewer for his important contributions to the early phases of this work and the National Institutes of Health for support under Grants HL-16860 (G.L.), GM-38401 (W.R.S.), and GM-23851 (C.A.R.).

(25) Sams, J. R.; Tsin, T. B. *Porphyrins* **1979**, *4*, 454.
(26) Gans, P.; Buisson, G.; Duee, E.; Marchon, J. C.; Erler, B. S.; Scholz, W. F.; Reed, C. A. *J. Am. Chem. Soc.* **1986**, *108*, 1223.
(27) Christner, J. A.; Munck, E.; Janick, P. A.; Siegel, L. M. *J. Biol. Chem.* **1983**, *258*, 1147.
(28) Saxton, R. J.; Olson, L. W.; Wilson, L. J. *J. Chem. Soc., Chem. Commun.* **1982**, 984.
(29) Brewer, G.; Wang, R. *J. Chem. Soc., Chem. Commun.* **1990**, 583.
(30) Matsumoto, N.; Okawa, H.; Kida, S.; Ogawa, T.; Ohyoshi, A. *Bull. Chem. Soc. Jpn.* **1989**, *62*, 3812.